Date: 23/10/03

FE modeling of bond interaction of FRP bars to concrete

Dr Zenon Achillides, *Scientific Associate*
National Technical University of Athens

Dr Kypros Pilakoutas, *Reader*
University of Sheffield

Contact address: Univ. of Sheffield, Dept. of Civil and Structural Eng., Sir Frederic Mappin Building, Mappin Street, Sheffield, S1 3JD, UK. Tel: +441142225065, Fax: +441142225700
email: k.pilakoutas@sheffield.ac.uk, zachillides@hotmail.com

No. of words: 4260

No. of tables/figures: 1/18

Synopsis:

In this paper a computational modeling approach is used to investigate the bond behaviour of FRP bars in concrete. Two Finite Element packages (ANSYS and ABAQUS) are used to model the bond interaction of FRP reinforcing bars in cubes and beams. The main purpose of this work is to develop additional understanding of how FRP bars "cooperate" with concrete to sustain the pullout load. Two modeling approaches are presented. In the first approach, a spring describing the behaviour of short embedment lengths in pullout tests was used for predicting the behaviour of longer embedment lengths. In the second approach, spring characteristics obtained from an experimentally determined bond stress versus anchorage length envelope are used in FE modeling of beams. Both approaches showed good agreement between analytical and experimental results. However, further development on the analytical modeling of the bond interaction is required, in order to consider the effect of all parameters that influence bond.

INTRODUCTION

Even though many experimental programs have been conducted worldwide examining the bond characteristics of FRP bars, relatively little work has been published on numerical modeling[1] of this type of bars. The use of available bond models developed for steel bars, can not offer the optimal solution, since FRP and steel have different material properties and bond failures. Hence, there is a pressing need for the development of analytical bond models based on the specific properties and modes of bond failure of FRP bars.

This paper will report some of the analytical work undertaken at the University of Sheffield as part of several EU funded projects[2] which investigated the use of non-ferrous reinforcement in RC structures. The main purpose of this work was to develop additional understanding of how FRP bars "cooperate" with concrete in each case in order to sustain the pullout load. Two experimental series were undertaken on bond. In the first series, more than 100 specimens were tested in direct pullout[3], whilst in the second, 37 concrete beams were tested to study the bond development along the FRP reinforcing bars[4]. The experience gained from the experimental work helped to enhance the understanding of bond behaviour of FRP bars to concrete and is used in the progress of modeling this behaviour.

EXPERIMENTAL ARRANGEMENT OF PULLOUT TEST

The FRP bars tested were produced during the development stages of the EUROCRETE project[2]. The bars consisted of around 70% of fibers, either Carbon or Glass, and 30% of resin. The surface deformations are created by the addition of a peel-ply on the surface of the bar during pultrusion, which is removed after the settlement and curing of the resin. This procedure created a rough external surface on the bar with an average peak height of 0.75 mm.

The bars that were tested in this experimental series had different types of cross-sectional areas, sizes and surface deformation textures. The Young's modulus of elasticity of the EUROCRETE FRP bars was evaluated by direct tension tests and the average values obtained are presented in Table 1 The supplier's characteristic tensile strength of the various bars are also given in the table.

Prior to casting, the FRP bars were properly marked so that the embedment length would lie in the middle of the concrete cube. The embedment lengths were designed as multiples of the bar diameter to facilitate comparisons among different diameter bars. The two ends of the bar in the concrete cube were wrapped with several layers of cling film to form non-contact (debonded) areas between bar and concrete in order to eliminate the "edge effect" of cube deformation on bond development. The bars were then positioned vertical in 150 mm cube moulds where concrete was cast around the bar. These bars where casted in concrete cubes (150 mm edge) and the pullout arrangement is shown in Fig. 1.

PULLOUT CUBE TEST MODEL

The cube test modeling procedure had two main objectives. The first objective was to help with the understanding of how the bond stress is developed at the FRP-concrete interface during pullout. This was not possible to be deducted from the experimental results since no strain gauges were attached on the embedment length of the bar in order not to disturb the bond development zone. The analytical results are intended to monitor the bond development during pullout on an FRP bar embedded in concrete. The second objective of the model is to help develop a procedure for predicting the bond behaviour of larger embedment lengths subjected to a pullout force, by using the experimental data from specimens with smaller embedment. This objective is considered to have practical usefulness since it is aimed in reducing the need of testing large numbers of specimens in order to establish the relationship of

how the average bond strength is influenced by an increase in the anchorage length[5] as it is accepted that the size of the embedment length influences the developed average bond strength on the bar[6].

The FE package ANSYS 5.0a[7] was used for modeling the bond behaviour of FRP bars in pullout cube tests. This package was preferred since it provides reliable elastic-analysis results. The analysis was conducted by using perfectly elastic materials (concrete and FRP), since concrete cracking was assumed to be of minor importance under the specific pullout experimental conditions. In addition, the elastic concrete model was favored since it provided a more stable solution, than the solution provided by a non-linear concrete model, which was needed for the investigation of the post-maximum bond behaviour of FRP bars. The results of the analytical study were compared to the experimental results gathered from the pullout tests[4]. The following analytical study concentrates mainly on the behaviour of GFRP 13.5 mm bars. However, the described procedure can be easily followed for investigating the bond behaviour of other types of reinforcing bars as far as sufficient amount of experimental pullout test data are available.

Description of the model

The FRP-concrete cube specimens were modeled by using 2-dimensional elements. The concrete was modeled by 4-noted plane square elements of 150 mm thickness and Young Modulus equal to 30 GPa, whereas 2-noted square bar elements of area 143.13 mm^2 and E=45 GPa were used to model the FRP bar. Bar and concrete were linked together with non-linear spring elements at a spacing of 27 mm (27 mm = 2 times the bar diameter). The use of this particular spacing is explained later, together with the characteristic load-slip curve of the springs. In order to model the different sizes of embedment length used in the experiments, 4 identical cube models were developed differing only in the number of connecting springs. Every spring was assumed to represent the bond contribution of a 27 mm bar length to the

overall bond behaviour of the embedment length. An example of modeling the G10D (GFRP 13.5 mm bar having embedment length = 10x D = 135 mm $\Rightarrow$ use of 5 springs) and the G6D specimen (GFRP 13.5 mm bar having embedment length = 6x D = 81 mm $\Rightarrow$ use of 3 springs) is presented in Fig. 2. The springs connect the bar point A with the concrete point B, both having the same coordinates with respect the origin O, although in figure they are shown to be remote from each other.

The model was constrained at the top face of the cube in the Y-direction, similar to the experimental set up. However, in order to avoid a differential movement of the model along the X-axis during pullout, the X-direction was also constrained at the left top corner of the model. The pullout load was applied on the bar in small increments along the Y-direction. This load was applied in deflection control, so that the study of the post-ultimate bond behaviour of the bar would be possible.

Spring characteristics

The main role of the spring elements in this model was to simulate the bond interaction between the bar and the surrounding concrete during pullout. The required input data that define the behaviour of the springs are the spring extension values and the corresponding force levels applied on the spring. In the case of this model, the spring extension was identified by the bond slip of the bar and the corresponding force was a function of the bond strength of the bar. In order to define the input load-bond slip curve, selected experimental data from the pullout cube tests were used. Fig. 3 shows the experimental load-unloaded end slip curves for four specimens having GFRP 13.5 mm embedded bars.

In order to explain the rationale of the springs' characteristics, the load versus unloaded end slip curves of the specimens G4D and G2D are considered in more detail. The 4D embedment length is assumed to be identical to two 2D lengths as shown in Fig. 4.

The unloaded end slip, δ_{ue}, is a function of the load F_1, which corresponds to the 4D embedment length, but is also a function of the internal load F_2 that corresponds to the bottom 2D embedment length. Since the load values F_1 and F_2 correspond to the *same* δ_{ue}, the difference between F_1 and F_2 will give a load value F that represents the contribution of the upper 2D length at that certain slip. The contribution of the upper 2D embedment to the Load-unloaded end slip curve of the whole 4D embedment, is the shaded area between the 4D and 2D curves. The resultant curve of F versus δ_{ue} is shown in Fig. 5. This curve was introduced in all the springs of the model except the very last one, where the F-δ_{ue} curve of the specimen G2D was used (see Fig. 3).

Results

All models failed in a pull-out mode of bond failure, without incurring any bar tensile failures. In order to examine the validity of the modeling procedure, the analytical results were compared with the corresponding experimental ones. In Fig. 6, the load-slip curves at the loaded (LE) and unloaded end (UE) of an embedded FRP bar in a concrete cube, having an embedment length 10 times the diameter of the bar (10D), are presented together with the respective experimental curves[3]. It should be reminded that the LE slips are greater than the UE slips since they incorporate the elongation of the embedment length of the bar. Fig. 6 shows that the analytical results follow closely the experimental results both at the loaded and unloaded end, which verifies the validity of the modeling procedure.

One of the main objectives of this analytical study is to monitor bond development during pullout on an FRP bar. Although the experimental data provide significant evidence of what is happening outside the embedment length (e.g. slip and load measurements), there are no data available that show how actually the bond is developed along the embedment length of the bar. This is an area where the analytical study can contribute towards a better understanding of the bond behaviour of FRP bars in concrete. Fig. 7 shows the normal and the

bond stress distributions along the embedment length, for the G10D model. At low load levels the peak bond stress is developed at the loaded end of the bar. As the pullout load increases, the bond stress seems to be constant along the whole embedment length. Close to the maximum pullout load (52 kN), the peak bond stress migrates towards the unloaded end of the cube, having a slightly higher value than the local bond value at the loaded end of the cube. After the maximum load, the bond stress values decrease over the whole embedment length until a certain load value where the bond behaviour of the bar is controlled by the frictional characteristics of the bar-concrete interface.

Prediction of the bond behaviour of larger embedment lengths

After predicting the bond behaviour for small embedment lengths ($L \leq 10D$), the modeling effort focused on relatively larger embedments. In this case, no experimental data were available for comparison purposes hence, the presented results are solely from the analytical study. Three larger embedments were examined having lengths equal to 297 mm (22D), 594 mm (44D) and 864 mm (64D). The bar-concrete connecting springs were placed at 27 mm intervals and the concrete cubes had larger dimensions than before. The geometry of one of these cubes for the embedment length of 22D is shown in Fig. 8.

The analytical results of the above pullout models showed that the bond strength of FRP bars decreases, as the embedment length increases. In Fig. 9, the maximum average bond strength is plotted against the embedment length. It is obvious that the rate of bond decrease is much faster in smaller embedments whereas for larger embedments the bond strength appears to be leveling off.

The distribution of normal and bond stresses along the embedment length as the pullout load increases, is shown in Fig. 10 for the 64D model. The peak bond stress initially develops at the loaded end of the bar and as the load increases, the peak value shifts towards the unloaded end. It can be deduced from the bond stress distribution graph that the contribution

of the peak bond stress to the average bond strength of the embedment appears to be more significant in smaller embedments, whereas for larger embedments the frictional bond stress is the critical parameter. This observation supports the findings of Fig. 9 that large embedments appear to have similar values of average bond strength since this value is more influenced by the value of frictional bond stress than the peak bond value. By considering the regression curve in Fig. 9, it can be suggested that in order to develop the full strength of a 13.5 mm GFRP EUROCRETE bar (estimated around 1000 MPa), an embedment length of around 945 mm (≅ 70D) is required. The average bond stress value at that length is equal to 3.6 MPa. It is important to note that up to this point no bond splitting is considered and the bar fails in a pull-through mode. In the following, a procedure is being described for modeling single bars in beam elements that fail due to bond splitting.

BEAM TEST SPLITTING MODEL

Examining the bond behaviour of reinforcement bars in beam elements was one of the main aims in this study. Their bond behaviour appears to differ from that in cube tests because of the different boundary conditions. Flexural cracks that develop in beam elements due to external loading, influence the bond development along the main reinforcing bars. In addition, bond failure in beam elements is usually due to concrete splitting which is different from the pull-through mode of failure in cube specimens. The main objective of this procedure is to model the behaviour of concrete beams tested in the experimental part of the EUROCRETE project that failed in bond splitting[8] and examine the bond development on the main reinforcing bars. For this reason, two beams are considered having similar reinforcement arrangement, as shown in Fig. 11, differing only the length of the single bar anchorage (L), which was 300 mm for one beam (beam CB32) and 580 mm for the other beam (beam CB37). In both cases the anchorage bar failed by splitting the concrete cover at the bottom face of the beam.

In order to model these two beams ABAQUS FE package[9] was used. ABAQUS was preferred than ANSYS, since it provides the facility of introducing a smeared-crack concrete model in 2-dimensional models. In addition, it is regarded to offer better non-linear solution procedures for approaching the initiation of cracking in the model. In the process of modeling the behaviour of these beams and more specifically the bond behaviour of the anchorage bars, the influence of the concrete splitting on the bond development had to be considered. For this reason, this modeling effort focused on introducing a working method of evaluating the bond splitting behaviour of the anchorage bars in beam elements.

Description of the models

Both beam models were reinforced with two 8 mm CFRP bars embedded in concrete. The additional anchorage bar that was supposed to fail in bond was connected to the concrete elements by using springs, as shown in Fig. 12. As in the experiments[8], GFRP shear links (10 mm x 4 mm cross section) were also modelled at a spacing of 75 mm. Different mesh dimensions were introduced in each model beam in order to facilitate the exact length of the anchorage bar. The selection of the mesh sizes was arbitrary since the modelling procedure used is believed to be insensitive to the spring size, and consequently the mesh size. As will be mentioned later, the analysis repeated by using different mesh sizes in order to examine the validity of this modelling procedure and the mesh sensitivity of the results.

The anchorage bar and the concrete elements were connected together with spring type elements. Although the procedure of determining the load-slip characteristics of the connecting springs was based on the previously described modelling knowledge (see pull-out test), some modifications were introduced in order to incorporate the splitting behaviour of the anchorage bar. It is known from literature that bond splitting occurs when there is no adequate concrete cover to the bar, at a lower bond value than the maximum bond strength of the bar. Fig. 13 shows a typical distribution of bond stress versus the *unloaded end slip* of an FRP bar, as it

was recorded during the experimental series of tests[4], together with an indicative bond splitting behaviour.

It is obvious that to model the bond splitting behaviour of the anchorage bar, the bond splitting strength (τ_{sp}) has to be quantified. For this reason, the bond values gathered from the experimental data of CB32 and CB37 beams were used[10].

Fig. 14 shows the average bond values developed on the anchorage bar of CB32 beam, at the time when the first splitting crack occurred at the bottom cover (similar graph was also obtained for beam CB37). Each value corresponds to the reading of one of the four strain gauges that were attached along the anchorage length of the bar. These values were calculated by using the strain gauge reading at that load level, divided by the distance of the gauge from the end of the bar. Non-linear regression was used to determine the tendency of these values, as indicated by the best-fit line. It has to be mentioned that due to gaps in the sequence of data the regression curve might not be very accurate. However, in the absence of any more experimental data from these or any other similar beams, it can be assumed that these distributions are valid for modelling purposes.

Based on the dimensions of the mesh (shown in Fig. 12), the appropriate τ_{sp} value was chosen for each type of spring from Fig. 14. This bond value was translated into a load value and was introduced in the spring characteristics. For example, for the mesh dimension 77.8 mm the value of τ_{sp} is 6.8 MPa. By applying this value to the fundamental bond relationship

$F = \tau * (\pi * d * L)$ where d is the bar diameter (8 mm) and L is 77.8 mm, the value of Load, F will be 13.2 KN.

The corresponding value of the unloaded end slip was assumed to be practically zero until the bond stress reaches quite high values close to the ultimate bond strength value. The experimental results reported in a previous study[3] confirmed this. The resulting load - slip

characteristic curves introduced in the anchorage length springs in beam CB32 are shown in Fig. 15.

Both models were reinforced with 8 mm CFRP Eurocrete bars having Young Modulus equal to 115 GPa whereas, the shear links had the elastic modulus of GFRP bars (E_G = 45 GPa). The concrete material characteristics introduced in the models were similar to the experimental ones and are shown in Fig. 16, together with the cylinder compressive stress (f_{cy}) - strain curve of the material.

Results

Both model beams failed due to bond failure. The results showed good agreement with the respective experimental, as shown in Table 2. The small differences between model and experimental values can be attributed to inaccuracies in the determination of the experimental splitting strength.

The load - midspan deflection curves together with the distribution of normal and bond stresses along the anchorage bar for both models are presented and compared with the respective experimental results, in Fig. 17 and Fig. 18. By examining the load-deflection curves of both beams, it can be said that they generally follow quite accurately the experimental ones, especially at low load levels. The difference at the ultimate load capacity can be attributed to the incapability of the model beams to sustain additional load after the slippage of the anchorage bar (convergence problems were created), whereas the experimental beams continued to sustain load with the remaining two main reinforcing bars.

The normal bar stress distribution graph of beam CB32 showed that the model predicted fairly accurately the stress value in the constant moment region (beyond 300 mm). However, in the shear span the experimental stress values appeared to be higher. Nevertheless, it has to be taken into account that the small number of springs used to model the anchorage in this model (only 3 springs) can not facilitate more detailed comparisons. Detailed comparisons

should not, also, be made for the distribution of bond stresses, although in this case the model curves (see for example curve Mod. 40kN) predicted quite well the respective experimental ones. Only the large bond value at the very end of the experimental curve could not be predicted by the model because of the relatively large spacing of the springs. By considering the normal and bond stress distribution in model CB37 beam, similar comments to the above can be made. However in this case, the larger anchorage length and the presence of more springs makes the comparison more accurate. The normal bar stresses both in the constant moment region and in the shear span were predicted quite accurately (see curves at 40 kN), although at higher load levels, close to the bar end, the experimental stress values appeared to be somewhat higher than the analytically predicted ones. This again can be attributed to the smeared crack approach of the FE package as opposed to the discrete cracking that develops in experimental conditions. Another interesting observation from the graphs of beam CB37 is that the distribution of model normal bar stresses is not as "smooth" as the experimental ones, which results to a non-smooth bond distribution along the bar. This is assumed to be related to the small mesh size used in the model that created dependence on the concrete flexural cracking. This, however, does not seem to influence the average bond behaviour of the bar, as it can be seen in the comparisons of the model results with the respective experimental. In addition, the results from modelling the same CB37 beam by using a larger mesh size also confirmed this statement[4]. These results showed that the modelling procedure described above does not depend on the spring size used.

Discussion on beam test splitting model

The analytical approach examined shows promise, since important behavioral aspects of reinforced concrete beams are well predicted. However, it is believed that to achieve further refinements, better constitutive models will have to be developed for modelling concrete in tension and shear. In particular, it is very important when dealing with bond on the micro level

to use a discrete crack approach since the effect of cracks was demonstrated in the experimental work to influence the bond demand in a very dramatic manner. CEB Bulletin[11] also confirms that flexural cracks appear to influence the development of bond on the bar. The negative and positive bond values developed between successive cracks in the cracked zone of the beam appear to reduce the average bond resistance in that region. As a result, the average bond developed in this zone is significantly lower than the bond in the uncracked zone. One approach of modelling this behaviour is to use different types of spring characteristics at the cracked and uncracked zone of the beam. This approach, however, although it might give satisfactory results, deals with bond macroscopically and does not consider the actual bond action on the bar. As a result, the various parameters that influence bond can not be incorporated in this approach since the spring values will always depend on specific experimental conditions.

An alternative approach to the problem might be to consider the concrete-bar system between successive cracks and examine in more detail the bond development at that region. In this case, the bar would still be connected with springs to concrete, but the springs would have to consider the variation in bond stress at the two crack edges. The results of this system have to be incorporated into an overall beam model, which uses the discrete crack approach to flexure. It is expected that this approach might be able to predict the peak bond values developed on the bar during loading, and give generally more reliable bond behaviour.

As a step further, the bond splitting failure might be able to be incorporated in the above modelling approach. In the method described in the previous paragraphs for modelling the bond splitting behaviour of beams CB32 and CB37, bond development was also examined macroscopically by taking the spring characteristics from tests on beams. Consequently, a dependence of the spring values on certain experimental conditions was apparent (i.e concrete cover, bar diameter etc). In order to eliminate this dependence, a more refined modelling

approach would have to be introduced. It is known that bond action is accompanied with radial stresses in the surrounding concrete, which might split the concrete cover[12]. Splitting, however, takes place in a plane perpendicular to the bar axis. So, the model would have to consider a relationship linking bond and radial stresses, so that a certain increase in bond would be accompanied with an increase of the radial stress in the transverse direction[13]. When this stress reaches the splitting strength of the concrete, a splitting crack would have to be developed and the bond strength of the bar would have to decrease. The above described approach would have to be incorporated in the bar-concrete system between successive cracks, so that an integrated solution should be developed.

In conclusion, it can be suggested that the modelling procedure described for beam elements enhanced the understanding of how actually bond develops between bar and concrete and highlighted modelling problems that will lead to the development of new approaches to bond splitting. One of these approaches was briefly described above and is expected to form a starting point for future research.

SUMMARY AND CONCLUDING REMARKS

A FE analytical study was conducted to investigate the bond behaviour of FRP bars in concrete. Pullout cube tests and selected beam tests were modelled by using ANSYS50a and ABAQUS FE packages. In the case of pullout tests, a modeling procedure was introduced where non-linear springs were used to model the bond behaviour at the bar-concrete interface. The basic spring characteristic load-slip curve was taken from the results of the experimental study. The analytical results showed a very good correlation with the respective experimental and helped to develop a further understanding of the bar-concrete interaction during pullout. As a step further, the above modeling procedure was used for evaluating the bond behaviour of larger embedment lengths when no bond splitting was expected.

In the case of beam tests, two beams were modelled that failed due to bond splitting. The smeared-crack concrete option of ABAQUS package was introduced in these models. Springs were used to simulate the bond behaviour at the bar-concrete interface. The smeared-crack approach used by the FE package was proved to be not so accurate in simulating the discrete flexural cracking in the experimental beams and resulted in differences in the bond development between experimental and model beams. However, the overall modeling results were compared with the respective experimental and showed, generally, a good agreement. Further development on the analytical modeling of the bond interaction is required, in order to consider the effect of concrete cover, transverse reinforcement and pressure, and shear transfer in concrete microcracks.

REFERENCES

1. *fib* bulletin 10, Bond of non-metallic reinforcement, *Chapter 7 in "Bond of Reinforcement in Concrete"*, State of the art report prepared by Task Group Bond Models, International Federation for Structural Concrete, Switzerland, 2000, 315-394
2. Pilakoutas K., Composites in Concrete Construction, *Failure Analysis of Industrial Composite Materials*, Gdoutos A., Pilakoutas K. and. Rodopoulos C. (Eds), McGraw-Hill Professional Engineering, 2000, 449-497
3. Achillides Z. and Pilakoutas K., Bond Behavior of FRP Bars under Direct Pullout Conditions, *Journal of Composites for Construction*, April 2004 (under publication Re: CC/2002/022298)
4. Achillides Z., Bond behaviour of FRP bars in concrete, *PhD Thesis, Centre for Cement and Concrete*, Dept. of Civil and Structural Engineering, The University of Sheffield, UK, 1998

5. Achillides Z., Pilakoutas K. and Waldron P., Modelling of FRP rebar bond behaviour, *3rd International Symposium on Non-Metallic (FRP) Reinforcement for Concrete Structures,* Sapporo, Japan, 1997, 423-430
6. Cosenza E., Manfredi G. and Realfonzo R., Behaviour and modelling of Bond of FRP rebars to concrete, *Journal of Composites for Construction*, 1997, Vol. 1, No. 2, 40-51
7. ANSYS version 5.0a, *Swanson Analysis Systems Inc*, 1992
8. Achillides Z. and Pilakoutas K., Bond behaviour of FRP reinforcing bars in concrete, *Proc. of conference "Bond in Concrete – from research to standards"*, Budapest, 2002
9. ABAQUS version 5.3, *Hibbit, Kalsson and Sorensen Inc*, 1993
10. Achillides Z., Pilakoutas K. and Waldron P., Bond behaviour of FRP bars to concrete, *3rd Int. Symp. on Non-Metallic (FRP) Reinforcement for Concrete Structures*, Sapporo, Japan, 1997, 341-348
11. Comite Euro-international du Beton Bulletin 151, *State-of-the-Art Report "Bond action and bond behaviour of reinforcement"*, 1982
12. Tepfers R., A theory of bond applied to overlapped tensile reinforcement splices for deformed bars, *Publication 73:2, Division of Concrete Structures, Chalmers University of Technology*, Goteborg, Sweden, 1973
13. Achillides Z. and Pilakoutas K., "Analytical approach to the bond behaviour of FRP bars in concrete", Procs of Conference "Bond in Concrete – from research to standards", Budapest, 20-22 Nov. 2002, pp. 700-707

LIST OF FIGURE CAPTIONS

Table 1 — Mechanical properties of FRP bars

Bar type	GFRP	CFRP
Young Modulus (MPa)	45000	115000
Tensile strength (MPa)	>1000	>1500

Table 2 — Comparison of model and experimental results

	Splitting Load (kN)	Normal bar stress at loaded end (MPa)	Beam deflection (mm)
Experim. CB32	45.5	553	18
Experim. CB37	80.6	861	30.2
Model CB32	43.9	512	15
Model CB37	84.2	926	27.7

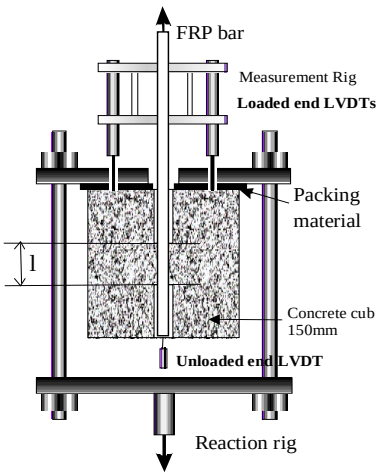

Fig. 1 — Experimental pullout arrangement

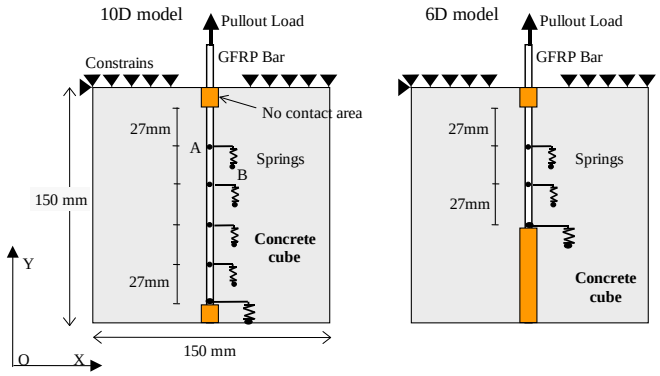

Fig. 2 — Spring model of G10D and G6D specimens

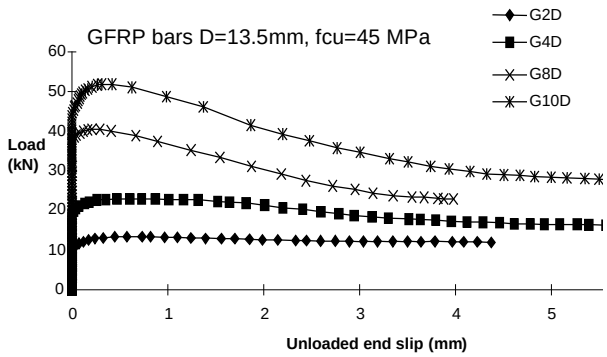

Fig. 3 — Experimental Load - Unloaded end slip curves of GFRP 13.5 mm bars

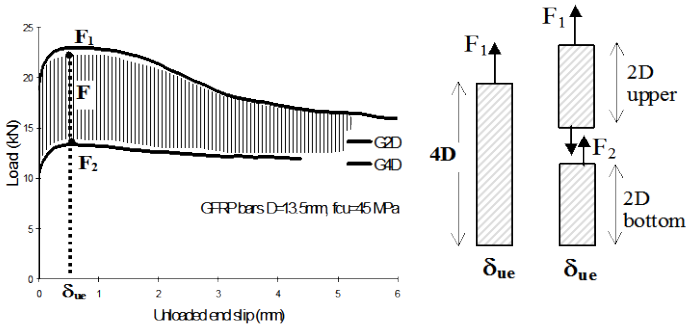

Fig. 4 — Contribution of the upper 2D bar length to the bond behaviour of the bar

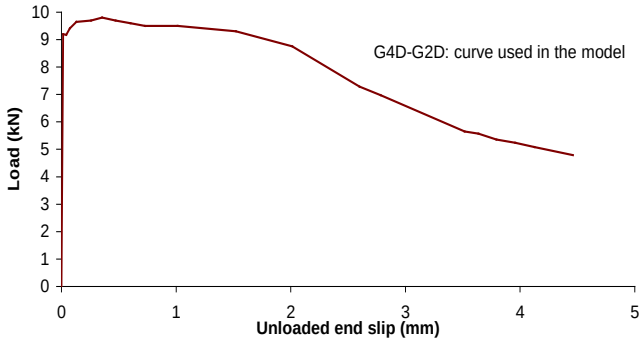

Fig. 5 — Load vs. unloaded end Slip for the "basic" embedment length (used for the modeling procedure)

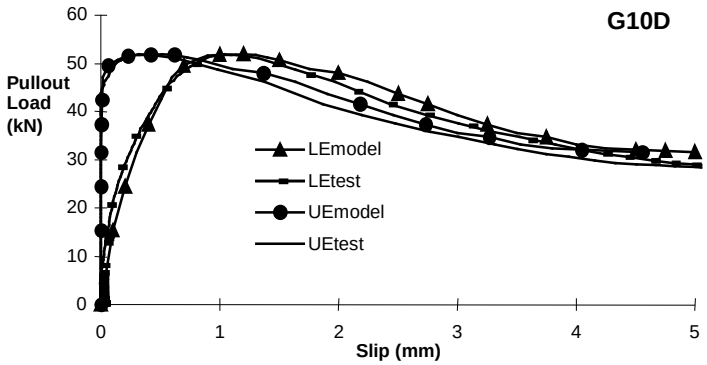

Fig. 6 — Load - slip curves of model and experimental test

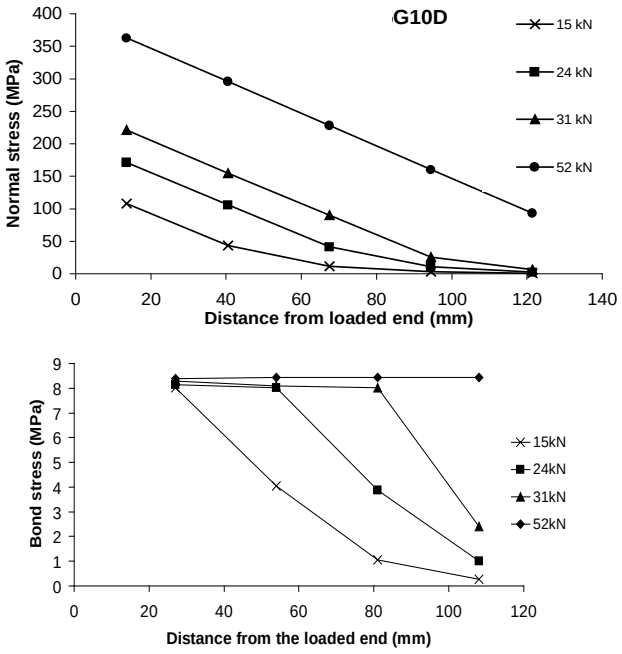

Fig. 7 — Normal and bond stress distribution along the embedment length of G10D model

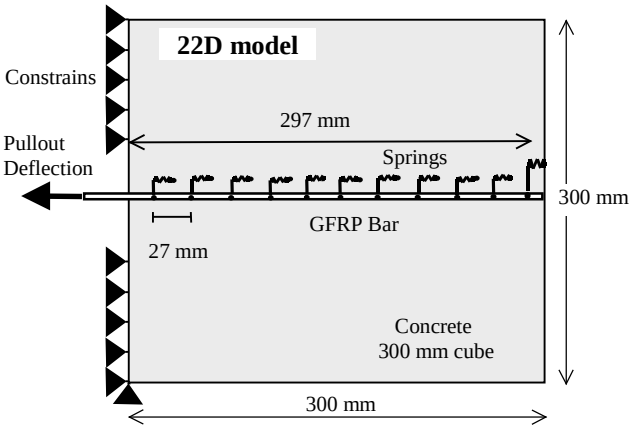

Fig. 8 — Model specimen of an embedment length equal to 22D (297 mm)

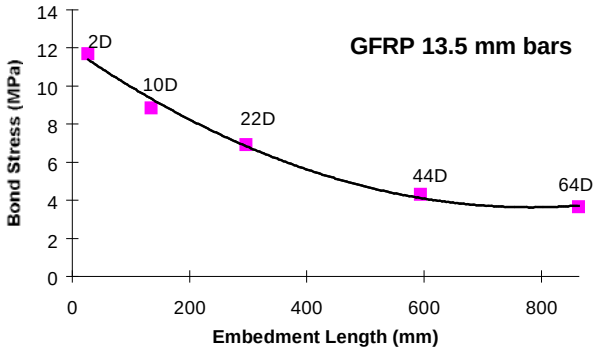

Fig. 9 — Maximum average bond strength versus embedment length for GFRP bars

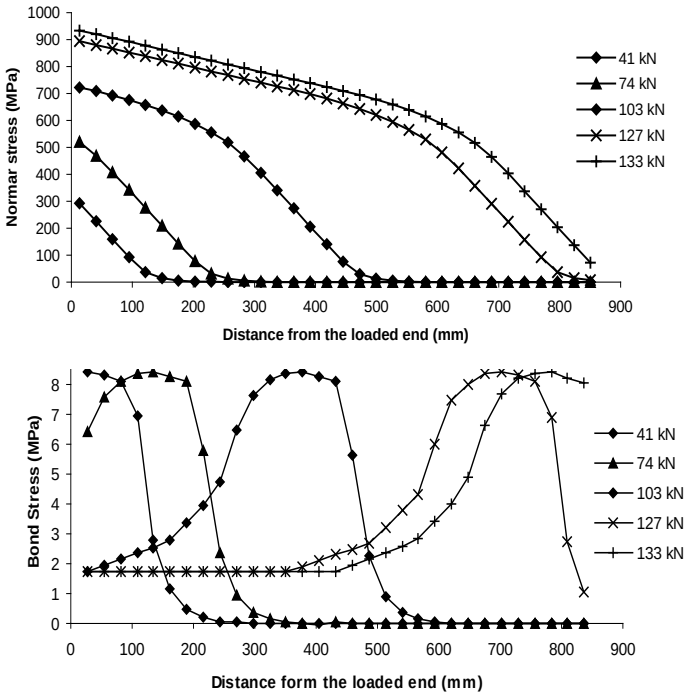

Fig. 10 — Normal bar stress and bond stress distributions along the 64D-embedment length

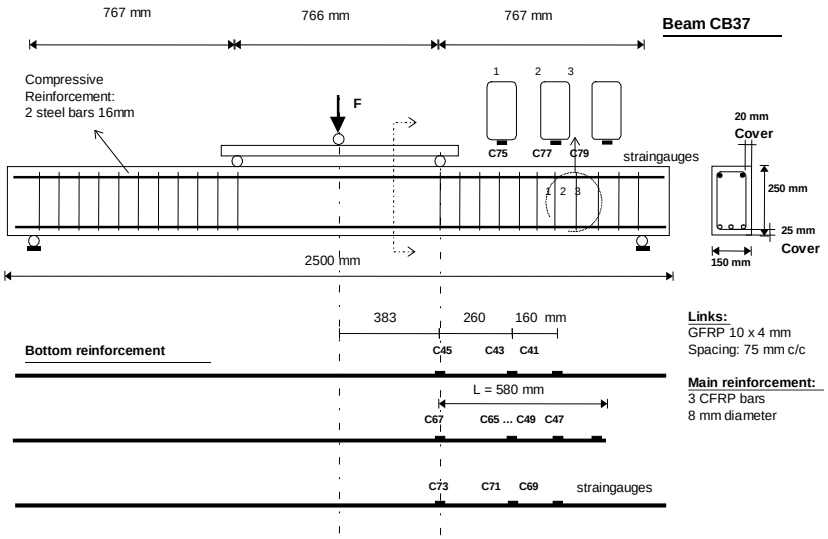

Fig. 11 — Reinforcement arrangement in the experimental series of beam tests (beam CB37)

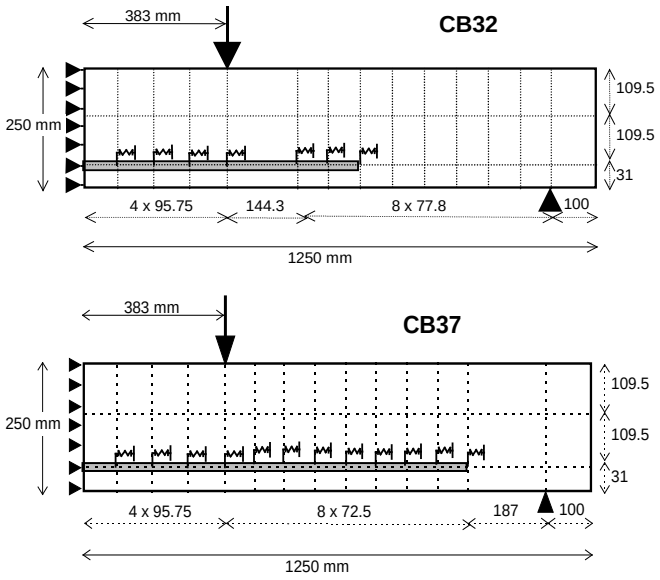

Fig. 12 — Models of CB32 and CB37 beams

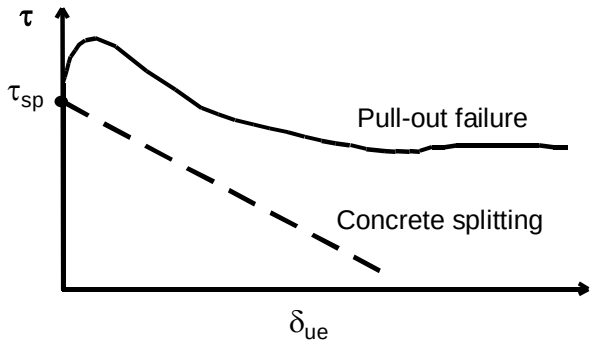

Fig. 13 — Indicative bond - unloaded slip curves for pullout and splitting bond failures

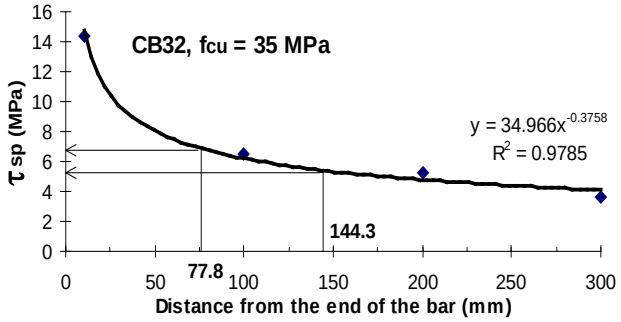

Fig. 14 — Average bond value developed at the time of splitting

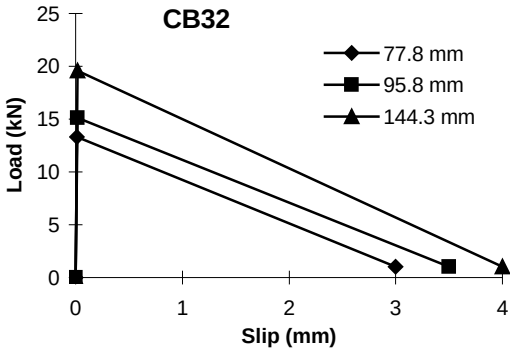

Fig. 15 — Characteristic load - slip curves introduced in the springs, in CB32 model

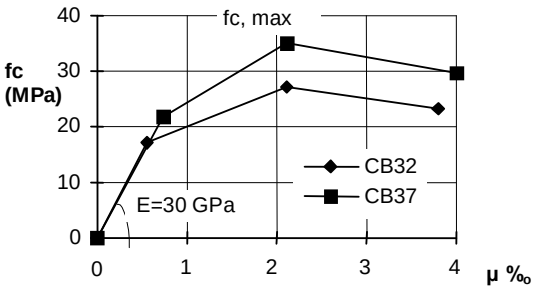

Fig. 16 — Concrete material characteristics

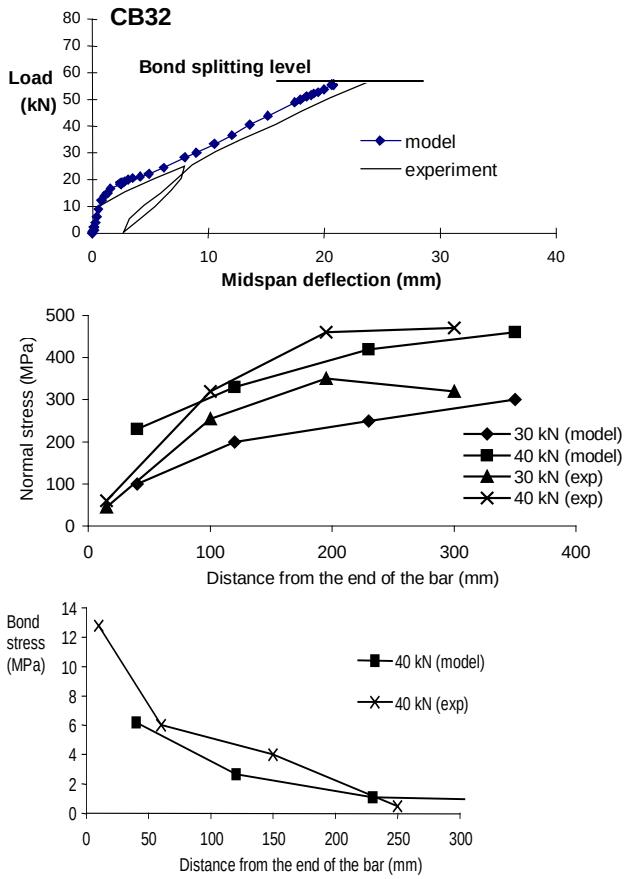

Fig. 17 — Load - deflection curve and normal and bond stress distributions for CB32

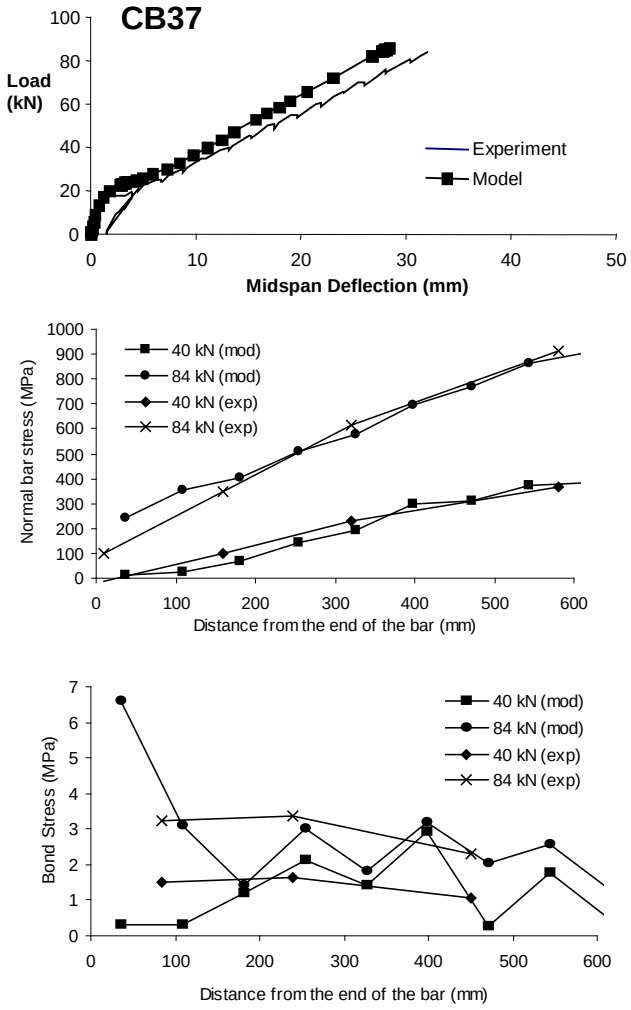

Fig. 18 — Load - deflection curve and normal and bond stress distributions for CB37